WALL PRESSURE FLUCTUATIONS IN A TURBULENT BOUNDARY LAYER AFTER BLOWING OR SUCTION

Joongnyon Kim, Kyoungyoun Kim, Hyung Jin Sung*
Department of Mechanical Engineering,
Korea Advanced Institute of Science and Technology
Gusong-dong, Yusong-gu, Daejon 305-701, Korea
jnkim@mail.kaist.ac.kr, kyoungyoun@mail.kaist.ac.kr, hjsung@mail.kaist.ac.kr

ABSTRACT

A direct numerical simulation of a spatially-developing turbulent boundary layer is performed to examine the characteristics of wall pressure fluctuations after the sudden application of wall blowing or suction. The uniform blowing or suction is given by the wall-normal velocity through a spanwise slot at the wall. The response of wall pressure fluctuations to uniform blowing or suction is analyzed by computing the turbulence statistics and frequency spectra. It is found that wall pressure fluctuations are more affected by blowing than by suction. The large elongated structure of wall pressure fluctuations is observed near the maximum location of $(p_w)_{rms}$ for blowing. The convection velocities for blowing increase with increasing the streamwise location after the slot. For both blowing and suction, the small scale of wall pressure fluctuations reacts in a short downstream distance to the spanwise slot, whereas the large scale recovers slowly in a farther downstream.

INTRODUCTION

The generation of wall pressure fluctuations is governed by the dynamics of velocity fluctuations throughout the entire boundary layer through a Poisson's equation. Wall pressure fluctuations at a local point in a turbulent boundary layer are coupled with global unsteadiness of associated flow structures. Practical interest in this subject arises because of undesired noise and vibration relevant to wall-bounded flows. Wavenumber-frequency spectra of wall pressure fluctuations are required as the forcing input function for structural models of flow-induced sound and vibration (Blake, 1986).

A literature survey reveals that most experimental and computational accounts on wall pressure fluctuations have been focused on equilibrium turbulent boundary layers over flat plates or inside channels. The first measurement of wall pressure fluctuations was made in a turbulent boundary layer over a flat plate by Willmarth (1956). He found that the ratio of r.m.s. wall pressure to dynamic pressure was approximately 0.0035. Bull (Bull, 1967) observed that wall pressure field has a structure produced by pressure sources with a wide range of convection velocities. A comprehensive overview of the role of wall pressure fluctuations was complied by Willmarth (1975). Recently, the statistical and spectral features of wall pressure fluctuations were obtained by direct numerical simulations (Choi and Moin, 1990) and by measurements with multi-arrayed pressure transducers (Lee and Sung, 1999).

*This work was supported by a grant from the National Research Laboratory of the Ministry of Science and Technology, Korea.

Relations of wall pressure fluctuations to near-wall coherent structures have also received extensive investigations in equilibrium turbulent boundary layers. By use of conditional average techniques, the velocity field structures related to high-amplitude wall pressure events were obtained experimentally (Thomas and Bull, 1983, Johansson et al., 1987). It was found that the shear-layer structures in the buffer region are responsible for the generation of high-amplitude wall pressure peaks. To study the structure of pressure fluctuations in turbulent channel flow, Kim (1989) decomposed the pressure into the rapid, slow and wall parts, and analyzed their contributions to various statistical quantities. The relationship between wall pressure fluctuations and streamwise vortices was examined by Kim et al. (2002a). They found that the generation of wall pressure fluctuations is closely linked with upstream stramwise vortices and turbulent kinetic energy production. In an effort to see the effects of pressure gradient and separation on the characteristics of wall pressure fluctuations, space-time correlation and frequency spectra of wall pressure fluctuations were examined by Na and Moin (1998), obtained from direct numerical simulation. They found that large two-dimensional roller-type structures are presented inside the separation bubble. Recently, Lee and Sung (2001, 2002) made a multiple-arrayed measurement of wall pressure fluctuations in a separated and reattaching flow over a backward-facing step. They found that there exist two modes of shed vortices by using unsteady wavelet analysis of wall pressure fluctuations.

Wall blowing or suction through a spanwise slot in a turbulent boundary layer has been frequently employed due to its potential possibility for turbulence control. Many direct numerical simulations were performed for testing the wall blowing or suction in a turbulent channel (Chung and Sung, 2001) and boundary layer flows (Park and Choi, 1999, Kim et al., 2002b). It is known that wall blowing gives rise to an upward shift in the mean velocity logarithmic law while a downward shift of the logarithmic velocity profile results from wall suction. The turbulent stresses are activated by wall blowing and decreased in the suction case. The wall pressure fluctuations can be affected significantly by the application of wall blowing or suction.

The objective of the present study is, therefore, to investigate the effects of wall blowing or suction on the characteristics of wall pressure fluctuations. Toward this end, a direct numerical simulation is made in a spatially-developing turbulent boundary layer. The Reynolds number based on the inlet momentum thickness (θ_0) and free stream velocity (U_∞) is $Re_\theta = 300$. The uniform blowing or suction is given by the wall-normal velocity through a spanwise slot at the wall (Kim et al., 2002b). Main emphasis is placed on the response of wall pressure fluctuations to sudden uniform

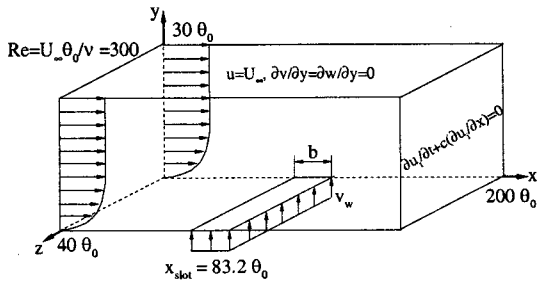

Figure 1: Schematic diagram of the computational domain.

blowing or suction. Turbulence statistics and frequency spectra of wall pressure fluctuations are obtained using standard techniques for stochastic data (Na and Moin, 1998). In order to deduce the spatial structure of wall pressure fluctuations, two-point correlation coefficients and several instantaneous fields are examined. Convection nature of wall pressure fluctuations is presented in terms of spatio-temporal correlations and convection velocities. Based on the wealth of DNS data, the source terms of the Poisson's equation are analyzed to investigate the contribution of each terms to wall pressure fluctuations.

NUMERICAL PROCEDURE

For an incompressible flow, the nondimensional governing equations are

$$\frac{\partial u_i}{\partial t} + \frac{\partial}{\partial x_j} u_i u_j = -\frac{\partial p}{\partial x_i} + \frac{1}{Re}\frac{\partial}{\partial x_j}\frac{\partial u_i}{\partial x_j}, \quad (i = 1, 2, 3), \quad (1)$$

$$\frac{\partial u_i}{\partial x_i} = 0, \quad (2)$$

where x_i are the Cartesian coordinates and u_i are the corresponding velocity components. All variables are nondimensionalized by a characteristic length and velocity scale, and Re is the Reynolds number.

The governing equations (1) and (2) are integrated in time by using a fully implicit decoupling method, which has been proposed by Kim et al. (2002c). All terms are advanced with the Crank-Nicolson method in time, and they are resolved with the second-order central difference scheme in space. Based on a block LU decomposition, both velocity-pressure decoupling and additional decoupling of the intermediate velocity components are achieved in conjunction with the approximate factorization (Kim et al. 2002c). The overall accuracy in time is second-order without any modification of boundary conditions. Since the decoupled momentum equations are solved without iteration, the computational time is reduced significantly.

A schematic diagram of the computational domain is illustrated in Fig. 1. Time-dependent turbulent inflow data are provided at the inlet based on the method by Lund et al. (1998). This approach is to extract instantaneous planes of velocity data from an auxiliary simulation of spatially-developing turbulent boundary layer. A plane velocity field near the domain exit is modified by the rescaling procedure and reintroduced to the inlet of the computational domain in

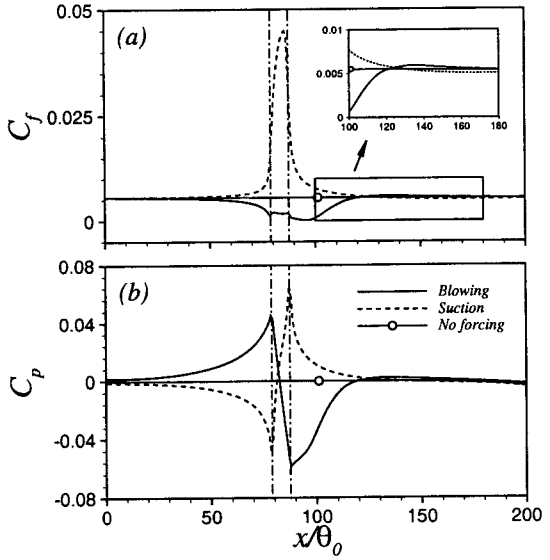

Figure 2: Streamwise distribution of mean variables at the wall: (a) skin friction coefficient; (b) wall pressure coefficient. Chain-dotted lines denote the location of the spanwise slot.

the inflow-generation simulation. The main simulation of developing turbulent boundary layer is then carried out in the range $0 \le x \le 200\theta_0$. Details regarding the numerical procedure of inflow generation are available in Lund et al. (1998). A convective boundary condition at the exit has the form $(\partial u_i/\partial t) + c(\partial u_i/\partial x) = 0$, where c is the local bulk velocity. The no-slip boundary condition is imposed at the solid wall, and the boundary conditions on the top surface of the computational domain are $u = U_\infty$ and $(\partial v/\partial y) = (\partial w/\partial y) = 0$. A periodic boundary condition is applied in the spanwise direction.

A spanwise slot for uniform blowing or suction is located from $x = 78.9\theta_0$ to $x = 87.5\theta_0$, where $x = 0$ corresponds to the inlet (Kim et al. 2002b). The slot width (b) is about $8.6\theta_0$. The magnitudes of uniform blowing ($v_w > 0$) or suction ($v_w < 0$) are 4.63% of the free stream velocity (U_∞), $|v_w| = 0.0463U_\infty$. The ratio of momentum flux gain/loss due to the blowing/suction and momentum flux of the incoming boundary layer ($\sigma = v_w b/U_\infty\theta_{slot}$) is 0.322, where θ_{slot} is the momentum thickness without blowing or suction at the slot location (Antonia et al. 1995).

The inlet Reynolds number based on the inlet momentum thickness (θ_0) and free stream velocity (U_∞) is $Re_\theta = 300$. The computational domain has dimensions $200\theta_0 \times 30\theta_0 \times 40\theta_0$ in the streamwise, wall-normal, and spanwise directions, respectively, which corresponds to $3200 \times 480 \times 640$ in wall units. The mesh contains $257 \times 65 \times 129$ points in the streamwise, wall-normal, and spanwise directions, respectively. The grid resolution is $\Delta x^+ \cong 12.5$, $\Delta y^+_{min} \cong 0.16$, $\Delta y^+_{max} \cong 24.1$, and $\Delta z^+ \cong 5.0$ in wall units based on the inlet friction velocity. Uniform grids are deployed in the streamwise and spanwise directions, and a hyperbolic tangent distribution is used for grids in the wall-normal direction. The computational time step used is $\Delta t^+ = 0.25$ and the total averaging time to obtain the statistics is $T_{avg} = 6250\nu/u_\tau^2$.

RESULTS AND DISCUSSION

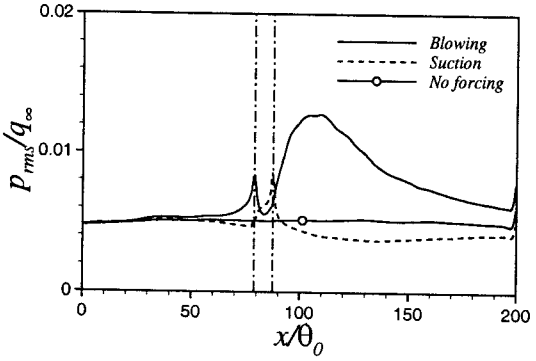

Figure 3: Streamwise distribution of the r.m.s. wall pressure fluctuations.

One-point statistics of wall pressure fluctuations

Before proceeding further, it would be advantageous to see the variations of mean variables along the wall. Figure 2 exhibits the streamwise distribution of skin friction (C_f) and wall pressure coefficient (C_p). For uniform blowing, the skin friction coefficient decreases rapidly near the slot. The adverse pressure gradient appears before and after the slot, whereas the favorable pressure gradient occurs above the slot. The opposite is observed for uniform suction. Overall characteristics of the mean wall variables are in good agreement with the previous results (Park and Choi, 1999, Kim et al. 2002b). It is known that when wall blowing is applied through a spanwise slot, streamwise vortices are lifted up with decreasing skin friction above the slot, whereas uniform suction diminishs turbulent fluctuations. However, the skin friction slightly increases in the downstream owing to the increased turbulent motion by uniform blowing (Park and Choi, 1999).

The streamwise distribution of r.m.s. wall pressure fluctuations $(p_w)_{rms}$ normalized by a reference dynamic pressure $q_\infty = \rho U_\infty^2/2$ is displayed in Fig. 3. For blowing, $(p_w)_{rms}$ increases significantly in the downstream, while decreases for suction. Although the magnitude of blowing velocity is equivalent to that of suction velocity, $(p_w)_{rms}$ of blowing changes more significantly than that of suction. Since high-amplitude wall pressure fluctuations are linked with streamwise vortices and turbulent kinetic energy production (Kim et al. 2002a), the activated streamwise vortices and turbulent fluctuations by the wall blowing may cause the increase of $(p_w)_{rms}$ in the downstream.

In order to examine the spectral features of wall pressure fluctuations, the frequency spectra of p_w are obtained using standard techniques for stochastic data (Na and Moin, 1998). The wall pressure fluctuations $p_w(x,z,t)$ are Fourier-transformed in the spanwise direction and time. Let $\hat{p_w}(x,k_z,\omega)$ be the discrete Fourier transform of $p_w(x,z,t)$, the power spectral density is computed by

$$\Phi(k_z,\omega;x) = < \hat{p_w}(x,k_z,\omega)\hat{p_w}^*(x,k_z,\omega) >, \qquad (3)$$

where (*) denotes complex conjugate and the bracket indicates an average over the spanwise direction and time. The dependence on the streamwise location x is considered from the flow inhomogeneity. The frequency spectra $\phi(\omega;x)$ are obtained by integrating $\Phi(k_z,\omega;x)$ over k_z. All spectra presented in this paper are normalized such that their integral is equal to the mean square of wall pressure fluctuations.

Owing to the different characteristics of velocity and length scales, a reliable similarity scaling law is important for the comparison of frequency spectra. The spectra obtained with the inner variable scaling, not shown in this paper, have a large discrepancy at all frequencies. Any scaling with friction velocity u_τ does not produce collapsed spectra in the presence of pressure gradient. As pointed out by Na and Moin (1998), this is due to the fact that u_τ is no longer an important parameter in boundary layers with pressure gradient.

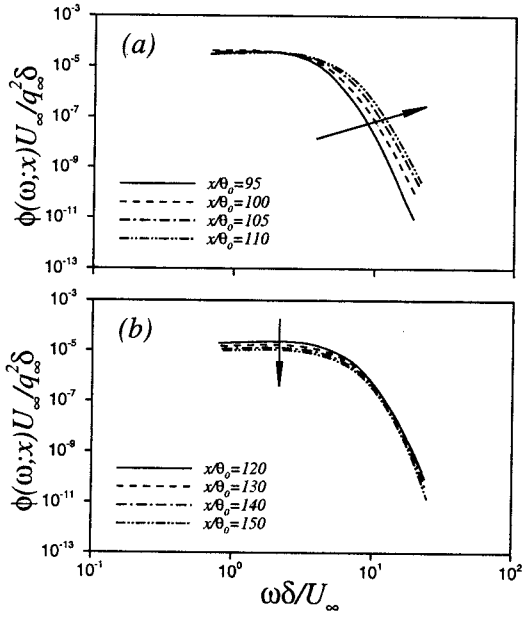

Figure 4: Frequency spectra of wall pressure fluctuations in the blowing case: (a) near the slot; (b) in the downstream.

The spectra normalized by the outer variables for blowing are illustrated in Fig. 4. Near the slot $x/\theta_0 < 110$, the spectra seem to collapse in the low frequencies and increase in the high frequencies with increasing the streamwise location x (Fig. 4(a)). An inspection of Fig. 4(a) discloses that the power in the high frequency region acts a main role on the increase of $(p_w)_{rms}$ for blowing. In the downstream $x/\theta_0 > 120$, the spectra in the low frequencies decrease with increasing x (Fig. 4(b)). This means that the decrease of large scale power gives the decrease of $(p_w)_{rms}$ in the downstream. For suction, the spectra decrease in the high frequencies with increasing x, indicating that the decrease of small scale power produces the decrease of $(p_w)_{rms}$. One could conclude from these spectra that the small scale of wall pressure fluctuations reacts quickly in a short downstream distance to both blowing and suction, whereas the large scale recovers slowly in a farther downstream.

Figure 5 shows the streamwise distribution of r.m.s. wall pressure fluctuations $(p_w)_{rms}$ normalized by the local maximum Reynolds shear stress $|\rho u'v'|_{max}$. It is seen that there is less variation of wall pressure fluctuations normalized by the local maximum Reynolds shear stress than by the reference dynamic pressure. This means that the maximum Reynolds shear stress $|\rho u'v'|_{max}$ appears to be a better scale to normalize wall pressure fluctuations in a locally-forced turbulent boundary layer. This scaling will be further investigated for the frequency power spectra of wall pressure fluctuations. However, the spiky discrepancy due to the non-fluctuating fluid injection is observed near the slot $x/\theta_0 < 100$. The injected fluid through the spanwise slot

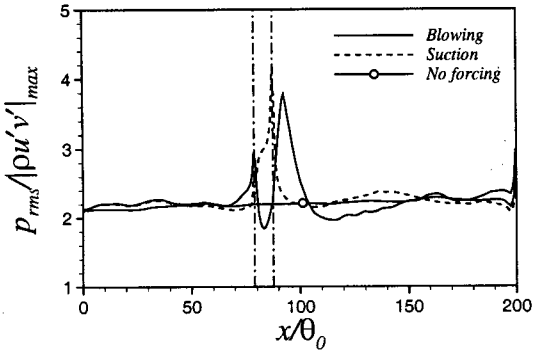

Figure 5: Streamwise distribution of the r.m.s. wall pressure fluctuations.

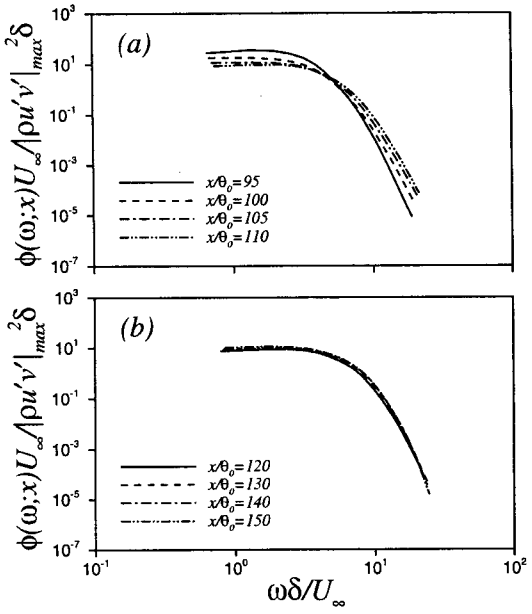

Figure 6: Frequency spectra of wall pressure fluctuations for blowing: (a) near the slot; (b) in the downstream.

has zero fluctuations, thereby affecting the velocity fluctuations and the Reynolds shear stress (Park and Choi, 1999, Kim et al. 2002b).

The frequency spectra normalized by the the maximum Reynolds shear stress $|\rho u'v'|_{max}$ with blowing are presented in Fig. 6. Except near the slot (Fig. 6(a)), this scaling produces a good collapse of the spectra at all frequencies (Fig. 6(b)). This means that the local maximum Reynolds shear stress has more direct influence on wall pressure fluctuations. However, the frequency spectra have a large discrepancy near the slot, at which the Reynolds shear stress can be affected by the non-fluctuating injected flow. Overall inspection of Figs. 5 and 6 discloses that the Reynolds shear stress $|\rho u'v'|_{max}$ is a better scale to normalize wall pressure fluctuations in a turbulent boundary layer.

Two-point correlations of wall pressure fluctuations

The spatial characteristics of wall pressure fluctuations are obtained from the two-point correlations as a function of the streamwise and spanwise spatial separations, which is defined between two locations separated by $(\Delta x, \Delta z)$ as

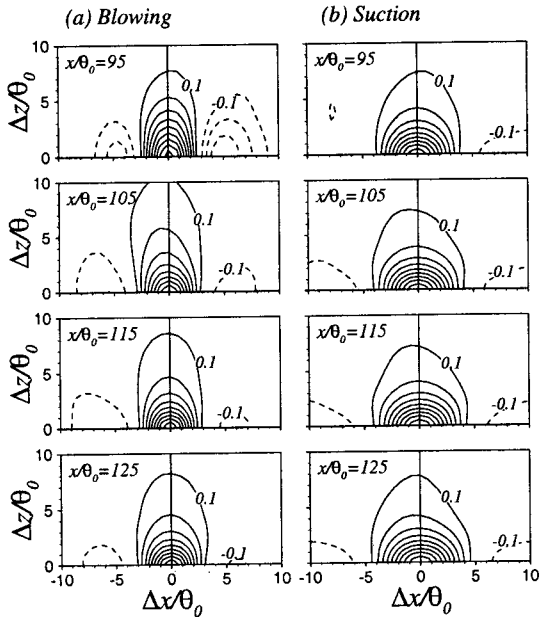

Figure 7: Contour of the two-point correlation of wall pressure fluctuations as a function of streamwise and spanwise separations: (a) blowing; (b) suction. Contour levels are from -0.3 to 0.9 with the increment of 0.1. Dashed lines denotes negative correlations.

$$R_{pp}(\Delta x, \Delta z; x) = \frac{< p_w(x,z,t) p_w(x+\Delta x, z+\Delta z, t) >}{p_{rms}(x,z,t) p_{rms}(x+\Delta x, z+\Delta z, t)}, \quad (4)$$

where the bracket indicates an average over the spanwise direction and time. Again, the dependence on the streamwise location x is considered from the flow inhomogeneity. Contour plots of the two-point correlation at four streamwise locations are presented in Fig. 7. For the purpose of comparison, the spatial separations are normalized by the inlet momentum thickness. For blowing, contours are elongated at larger separations in the spanwise direction (Fig. 7(a)). The spanwise extent of the widest contour corresponding to the contour level 0.1 increases up to $x/\theta_0 = 105$, at which $(p_w)_{rms}$ has the maximum value. This indicates that the integral length scale of wall pressure fluctuations increases near the slot region.

The large elongated structure of wall pressure fluctuations is clearly seen in a top view of a time sequence in the evolution of wall pressure fluctuations. The spanwise extended structure is observed near the maximum location of $(p_w)_{rms}$ in the several instantaneous fields. As will be shown the next section, this is due to the strengthened vortical structure, which produces the wall-normal motions in the buffer region and the relevant spanwise spread beneath the viscous sublayer. However, the contours for suction have little change.

Figure 8 shows the two-point correlation of wall pressure fluctuations as a function of the streamwise spatial and temporal separations, which is given by

$$R_{pp}(\Delta x, \Delta t; x) = \frac{< p_w(x,z,t) p_w(x+\Delta x, z, t+\Delta t) >}{p_{rms}(x,z,t) p_{rms}(x+\Delta x, z, t+\Delta t)}. \quad (5)$$

Here, the bracket indicates an average over the spanwise direction and time. Strong convection nature of the wall pressure fluctuations is seen by the concentration of the con-

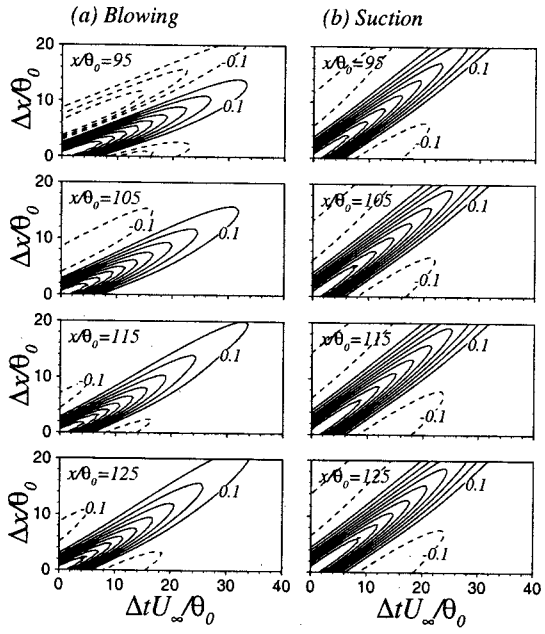

Figure 8: Contour of the two-point correlation of wall pressure fluctuations as a function of streamwise spatial and temporal separations: (a) blowing; (b) suction.

tours in a band. A slight increase in the slope of $\Delta x^+/\Delta t^+$ indicates that the convection velocity of large eddies is higher than that of small eddies. Furthermore, the slope of the contour with blowing increases with increasing the streamwise location x (Fig. 8(a)), whereas it has little change with suction (Fig. 8(b)). This means that the convection velocities of wall pressure fluctuations increase with increasing x near the slot region for blowing.

Analysis of pressure source terms

The Poisson's equation for pressure fluctuations is derived by taking the divergence of equation (1). By decomposing the velocity field into mean and fluctuations as $u_i = U_i + u_i'$, the equation can be written as,

$$\frac{\partial^2 p}{\partial x_i \partial x_i} = -\left\{ 2\frac{\partial U_i}{\partial x_j}\frac{\partial u_j'}{\partial x_i} + \frac{\partial^2}{\partial x_i \partial x_j}\left(u_i'u_j' - \overline{u_i'u_j'}\right)\right\}, \quad (6)$$

where x_i are the Cartesian coordinates, u_i are the corresponding velocity components and overbar indicates an average over the spanwise direction and time. The first term on the right-hand side is the mean-shear (MS) source term ("linear" or "rapid"), whereas the other term represents the sum of the turbulence-turbulence (TT) source term ("nonlinear" or "slow"). The MS and TT terms are given by

$$T^{MS} = 2\frac{\partial U_i}{\partial x_j}\frac{\partial u_j'}{\partial x_i}, \quad (7)$$

$$T^{TT} = \frac{\partial^2}{\partial x_i \partial x_j}(u_i'u_j' - \overline{u_i'u_j'}). \quad (8)$$

For the present boundary layer, the spanwise mean velocity gradient is zero. Among the linear source terms T^{MS}, $2(\partial U/\partial y)(\partial v'/\partial x)$ is about $50-100$ times larger than any other MS terms. The TT source terms can be written as

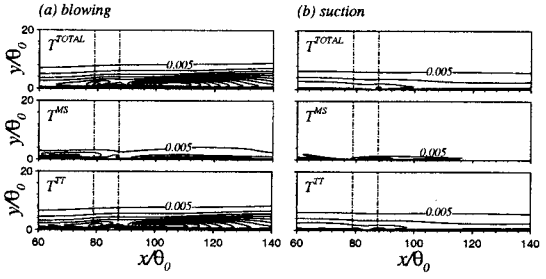

Figure 9: Contours of the r.m.s. source terms: (a) blowing; (b) suction. Contour levels are from 0.005 to 0.07 with the increment of 0.005.

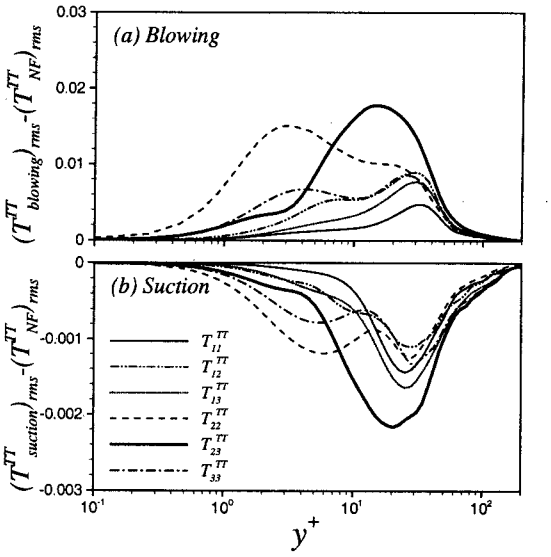

Figure 10: Profiles of the r.m.s. TT terms; (a) blowing; (b) suction.

$$T_{11}^{TT} = \left(\frac{\partial u'}{\partial x}\right)^2 - \frac{\partial^2}{\partial x^2}\overline{u'^2}, \quad (9)$$

$$T_{12}^{TT} = T_{21}^{TT} = \frac{\partial v'}{\partial x}\frac{\partial u'}{\partial y} - \frac{\partial^2}{\partial x \partial y}\overline{u'v'}, \quad (10)$$

$$T_{13}^{TT} = T_{31}^{TT} = \frac{\partial w'}{\partial x}\frac{\partial u'}{\partial z}, \quad (11)$$

$$T_{22}^{TT} = \left(\frac{\partial v'}{\partial y}\right)^2 - \frac{\partial^2}{\partial y^2}\overline{v'^2}, \quad (12)$$

$$T_{23}^{TT} = T_{32}^{TT} = \frac{\partial w'}{\partial y}\frac{\partial v'}{\partial z}, \quad (13)$$

$$T_{33}^{TT} = \left(\frac{\partial w'}{\partial z}\right)^2, \quad (14)$$

where x, y, and z denote the Cartesian coordinates and u, v, and w are the corresponding velocity components, respectively.

Contours of the r.m.s. source terms from equations (7) and (8) are shown in Fig. 9. For both blowing (Fig. 9(a)) and suction (Fig. 9(b)), r.m.s. of the nonlinear source term T^{TT} is much larger than that of the linear source term T^{MS} throughout the boundary layer. This is because $\partial u_j'/\partial x_i$ is rather small in the present turbulent boundary layer with blowing or suction. Furthermore, the r.m.s. source terms are much activated by blowing (Fig. 9(a)) than by suction (Fig. 9(b)), even though the velocities of blowing or suction are the same. This means that the pressure source terms of

the Poisson's equation are much more affected by blowing than by suction.

To obtain further insight of the nonlinear source term T^{TT}, the profiles of the nonlinear source terms for blowing or suction are shown in Fig. 10. For comparison, the difference between the r.m.s. source term for blowing or suction and the term without blowing or suction is presented. For bowing (Fig. 10(a)), $T_{23}^{TT} = (\partial v'/\partial z)(\partial w'/\partial y)$ has the largest r.m.s. value near $y^+ = 20$, which corresponds to the average location of the center of streamwise vortices. Note that $T_{22}^{TT} \cong (\partial v'/\partial y)^2$ has the largest value in the viscous sublayer near $y^+ = 5$, which would be related to the wall-normal motions like sweep or ejection. A closer inspection of Fig. 10 indicates that the second largest term in the viscous sublayer is $T_{33}^{TT} = (\partial w'/\partial z)^2$, which is due to a high spanwise gradient as the flow spreads out. In summary, the activated streamwise vortices and the relevant motions in the viscous sublayer are responsible for the increase of wall pressure fluctuations and the generation of large-elongated structures. On the other hand, when uniform suction is applied, the strength of the r.m.s. source terms are weakened. Note that the difference of the source terms for blowing (Fig. 10(a)) is about 10 times larger than that for suction (Fig. 10(b)). This means that the pressure source terms are 10 times more affected by blowing than by suction for the same blowing or suction velocities.

CONCLUSIONS

A detailed numerical analysis has been performed to delineate the characteristics of wall pressure fluctuations in a turbulent boundary layer with uniform blowing or suction. The statistical descriptions of wall pressure fluctuations were obtained by performing a direct numerical simulation of a spatially-developing turbulent boundary layer. When uniform bowing is applied from a spanwise slot, lifted and strengthened quasi-streawise vortices paly a main role in the increase of the magnitude of the non-linear source terms in the Poisson's equation. In particular, T_{23}^{TT} increases in the buffer region, which is related to ω_x, whereas the T_{22}^{TT} and T_{33}^{TT} terms increase in the viscous sublayer owing to the relevant resulting motions beneath the vortices. The opposite is observed for suction. The increasing rate by blowing is of the order of about 10 times larger than the decreasing rate by suction. Although the magnitude of blowing velocity is equal to that of suction velocity, $(p_w)_{rms}$ of blowing changes more significantly than that of suction. Owing to the relevant motions beneath quasi-streamwise vortices, the large elongated structure of wall pressure fluctuations is observed near the maximum location of $(p_w)_{rms}$ for blowing. For both blowing and suction, the small scale of wall pressure fluctuations reacts in a short downstream distance to the spanwise slot, whereas the large scale recovers in a farther downstream. The Reynolds shear stress $|\rho u'v'|_{max}$ is a better scale to normalize wall pressure fluctuations.

REFERENCES

Antonia, R. A., Zhu, Y., and Sokolov, M., 1995, "Effect of concentrated wall suction on a turbulent boundary layer", *Phys. Fluids*, Vol. 7, pp. 2465.

Blake, W. K., 1986, "Mechanics of flow-induced sound and vibration", Academic Press, INC.

Bull, M. K., 1967, "Wall pressure fluctuations associated with subsonic turbulent boundary layer flow", *J. Fluid Mech.*, Vol. 28, pp. 719.

Choi, H. and Moin, P., 1990, "On the space-time characteristics of wall-pressure fluctuations", *Phys. Fluids*, Vol. A2(8), pp. 1450.

Chung, Y. M. and Sung, H. J., 2201, "Initial relaxation of spatially-evolving turbulent channel flow subjected to sudden wall blowing and suction", *AIAA J.*, Vol. 39, pp. 2091.

Johansson, A. V., Her, J. -Y., and Haritonidis, J. H., 1987, "On the generation of high-amplitude wall-pressure peaks in turbulent boundary layers and spots", *it J. Fluid Mech.*, Vol. 175, pp. 119.

Kim, J., 1989, "On the structure of pressure fluctuations in simulated turbulent channel flow", *J. Fluid Mech.*, Vol. 205, pp. 421.

Kim, J., Choi, J.-I., and Sung, H. J., 2002a, "Relationship between wall pressure fluctuations and streamwise vortices in a turbulent boundary layer", *Phys. Fluids*, Vol. 14, pp. 898.

Kim, K., Sung, H. J., and Chung, M. K., 2002b, "Assessment of local blowing and suction in a turbulent boundary layer", *AIAA J.*, Vol. 40, pp. 175.

Kim, K., Baek, S.-J., and Sung, H. J., 2002c, "An implicit velocity decoupling procedure for the incompressible Navier-Stokes equations", *Int. J. Numerical Methods in Fluids*, Vol. 38, pp. 125.

Lee, I. and Sung, H. J., 1999, "Development of an array of pressure sensors with PVDF film", *Exp. Fluids*, Vol. 26, pp. 27.

Lee, I. and Sung, H. J., 2001, "Characteristics of wall pressure fluctuations in separated and reattaching flows over a backward-facing step: Part II. Unsteady wavelet analysis", *Exp. Fluids*, Vol. 30, pp. 273.

Lee, I. and Sung, H. J., 2002, "Multiple-arrayed pressure measurement toward the investigation of the unsteady flow structure of a reattaching shear layer over a backward-facing step", *J. Fluid Mech.*, Vol. 463, pp.377.

Lund, T. S., Wu, X., and Squires, K. D., 1998, "Generation of turbulent inflow data for spatially-developing boundary layer simulations", *J. Comput. Phys.* Vol. 140, pp. 233.

Na, Y. and Moin, P., 1998, "The structure of wall-pressure fluctuations in turbulent boundary layers with adverse pressure gradient and separation", *J. Fluid Mech.*, Vol. 377, pp. 347.

Park, J. and Choi, H., 1999, "Effects of uniform blowing or suction from a spanwise slot on a turbulent boundary layer flow", *Phys. Fluids*, Vol. 11, pp. 3095.

Willmarth, W. W., 1956, "Wall pressure fluctuations in a turbulent boundary layer", *J. Acoust. Soc. Am.*, Vol. 28, pp. 1048.

Willmarth, W. W., 1975, "Pressure fluctuations beneath turbulent boundary layers", emphAnn. Rev. Fluid Mech., Vol. 7, pp. 13.

Thomas, A. S. W. and Bull, M. K., 1983, "On the role of wall pressure fluctuations in deterministic motions in the turbulent boundary layer", *J. Fluid Mech.*, Vol. 128, pp. 283.